The crystal structure of D-lactate dehydrogenase, a peripheral membrane respiratory enzyme

Orly Dym*, Elizabeth Ann Pratt†, Chien Ho†, and David Eisenberg*‡§¶‖

*Department of Energy Laboratory of Structural Biology and Molecular Medicine, ‡Department of Chemistry and Biochemistry, §Molecular Biology Institute, and ¶Department of Biological Chemistry, University of California, Los Angeles, CA 90095; and †Department of Biological Sciences, Carnegie Mellon University, 4400 Fifth Avenue, Pittsburgh, PA 15213

Contributed by David Eisenberg, June 6, 2000

D-Lactate dehydrogenase (D-LDH) of *Escherichia coli* is a peripheral membrane respiratory enzyme involved in electron transfer, located on the cytoplasmic side of the inner membrane. D-LDH catalyzes the oxidation of D-lactate to pyruvate, which is coupled to transmembrane transport of amino acids and sugars. Here we describe the crystal structure at 1.9 Å resolution of the three domains of D-LDH: the flavin adenine dinucleotide (FAD)-binding domain, the cap domain, and the membrane-binding domain. The FAD-binding domain contains the site of D-lactate reduction by a noncovalently bound FAD cofactor and has an overall fold similar to other members of a recently discovered FAD-containing family of proteins. This structural similarity extends to the cap domain as well. The most prominent difference between D-LDH and the other members of the FAD-containing family is the membrane-binding domain, which is either absent in some of these proteins or differs significantly. The D-LDH membrane-binding domain presents an electropositive surface with six Arg and five Lys residues, which presumably interacts with the negatively charged phospholipid head groups of the membrane. Thus, D-LDH appears to bind the membrane through electrostatic rather than hydrophobic forces.

Membrane proteins have been broadly classified as integral or peripheral (1). Originally the distinction was based on the difficulty or ease of extraction of the protein from lipid. During the past decade, the molecular determinants of each class have gradually emerged through x-ray structures of roughly a dozen members of each class. Integral membrane proteins are now usually considered to be those that penetrate both leaflets of the lipid bilayer. They have a high proportion of apolar residues, particularly in the segments that are embedded in the apolar center of the membrane. Polar residues may also interact with polar head groups. Peripheral membrane proteins tend to penetrate only one leaflet of the bilayer. The intermolecular forces that adhere these proteins to the lipid may be a combination of hydrophobic and electrostatic forces, or in some cases may be mainly electrostatic forces. In the case of mainly electrostatic forces, the peripheral membrane proteins display an electropositive surface, composed of Arg and Lys residues, which presumably interacts with electronegative phospholipid head groups (2, 3). In the case of both hydrophobic and electrostatic forces, the peripheral membrane protein can contain an apolar α helix that penetrates into a single leaflet (4), or more often apolar loops distributed on one surface of the protein that penetrate the hydrophobic interior of the membrane (5). In both cases, polar residues interact with the phospholipid head groups.

Some respiratory proteins contain integral membrane subunits (e.g., succinate dehydrogenase, fumarate reductase), and others are peripheral membrane proteins [e.g., D-lactate dehydrogenase (D-LDH)]. These respiratory enzymes oxidize a variety of organic substrates (e.g., formate, succinate, lactate), passing the electrons to a variety of oxidants (e.g., oxygen, nitrate, fumarate). The free energy available from these reactions is used by other membrane proteins to do work, such as solute transport or ATP synthesis. *Escherichia coli* uses D-lactate as a carbon source and subsequently transfers two electrons and two protons to the electron transfer chain (6, 7). The electron acceptor is quinone, and all of the reactions occur on the cytoplasmic surface of the inner membrane.

Detergent is required for isolation and purification of D-LDH, and the enzymatic activity is enhanced by a variety of detergents and lipids (8, 9). However, D-LDH can be eluted from *E. coli* membranes by washing with 0.6 M guanidine hydrochloride (10), and its amino acid composition is not particularly apolar, which suggests that D-LDH, like some other primary dehydrogenases involved in electron transfer in *E. coli*, is a peripheral rather than an integral membrane protein. D-LDH consists of a single protein chain of 571 amino acid residues (65 kDa) and has the characteristic yellow color of the noncovalently bound flavin adenine dinucleotide (FAD) cofactor.

The kinetics of the enzyme were investigated by using stopped-flow spectroscopy (11). The reduction of D-LDH by the substrate, D-lactate, exhibits two stages. The fast stage represents the rapid formation of the enzyme–substrate complex, and the slow stage represents the slow release of the product, pyruvate, from the reduced enzyme. An anionic D-LDH semiquinone (one electron reduced) was observed and identified by using optical and electron paramagnetic resonance spectroscopy during the oxidation of the reduced enzyme by nitroxide-spin labels (11). On the basis of the structure, we propose a pathway of electron transfer from the FAD molecule via the electron acceptor quinone to the membrane.

Coupled site-specific mutagenesis and ^{19}F-NMR spectroscopy were used to investigate the properties of D-LDH (12–15). 5-Fluorotryptophan was incorporated into the native enzyme, which contains five tryptophan residues, and into mutant enzymes, where a sixth tryptophan was substituted into a specific site. The ^{19}F-NMR signal from the native and substituted Trp residues reported their sensitivity to substrate, exposure to aqueous solvent, and proximity to the phospholipid. The membrane-associated regions of the protein were found to be between residues Tyr-228 and Phe-369. Residues sensitive to both D-lactate and oxalate, a competitive inhibitor, were found at residues 139–144 (G. R. Matcuk, Jr., E.A.P. & C.H., unpublished results).

D-LDH belongs to a recently discovered family of FAD-dependent proteins (16) that share conserved residues in their FAD-binding domain. Some of the family members are vanillyl-alcohol oxidase (16), *p*-cresol methylhydroxylase (PCMH) (17),

Abbreviations: D-LDH, D-lactate dehydrogenase; FAD, flavin adenine dinucleotide; MurB, UDP-*N*-acetylenolpyruvylglucosamine reductase; PCMH, *p*-cresol methylhydroxylase.

Data deposition: The atomic coordinates and structure factors have been deposited in the Protein Data Bank, www.rcsb.org (PDB ID code 1F0X).

‖To whom reprint requests should be addressed at: University of California, Department of Energy Laboratory of Structural Biology, 201 MBI Building, Box 951570, Los Angeles, CA 90095-1570. E-mail: david@mbi.ucla.edu.

The publication costs of this article were defrayed in part by page charge payment. This article must therefore be hereby marked "*advertisement*" in accordance with 18 U.S.C. §1734 solely to indicate this fact.

Table 1. Summary of x-ray data collection from crystals of selenomethionine D-LDH

	Se peak	Se inflection	Se remote
Resolution, Å	20–1.9	20–1.9	20–1.9
λ, Å	0.97851	0.97880	0.97116
Total reflections	1,154,879	1,157,334	1,148,628
Unique reflections	95,767	95,814	95,259
Completeness, %	91.1	91.1	92.1
R_{sym}*, %	8.1	7.0	7.3
I/σ	20.3	24.3	22.8

*$R_{sym} = \Sigma_{i(h,k,l)} |I_{i(h,k,l)} - \langle I_{(h,k,l)} \rangle| / \Sigma_{i(h,k,l)} \langle I_{(h,k,l)} \rangle$, where $\langle I_{(h,k,l)} \rangle$ is the statistically weighted average intensity of symmetry equivalent reflections.

and UDP-*N*-acetylenolpyruvylglucosamine (MurB) (18). These proteins are found in both eukaryotes and eubacteria and catalyze a diverse range of redox reactions in a wide variety of metabolic pathways. The most prominent difference between the structure of D-LDH and the structure of other proteins from this FAD family lies in the membrane-binding domain. On the basis of these structural differences and in comparison to structures of other peripheral membrane proteins, we propose a model for D-LDH association with the membrane.

Materials and Methods

Protein Crystallization and Data Collection. The D-LDH protein used for crystallization was a mutant, K368W, which was selected as more stable than the native protein. Crystals of D-LDH in the presence of FAD were grown by the hanging drop vapor diffusion method from 3–5% (wt/vol) polyethylene glycol, molecular weight 4,000 Da (PEG 4000), and 0.1 M sodium acetate, pH = 5.2. Crystals of selenomethionine-substituted D-LDH were grown similarly, but PEG 6000 was used instead of PEG 4000. Crystals formed in space group $P2_1$, with cell constants a = 69.13 Å, b = 77.15 Å, c = 100.30 Å, β = 96.11°, and contain two monomers in the asymmetric unit. The selenomethionine crystals were flash cooled at 99 K with 30% PEG 6000 as a cryoprotectant. The multiple-wavelength anomalous diffraction data from a single crystal were collected at the National Synchrotron Light Source beamline X8C by using a MAR-CCD detector. Bijvoet pairs to 1.9 Å resolution were collected at the LIII absorption edge (λ_1 = 0.9785 Å, maximal $\Delta f''$), at the inflection point (λ_2 = 0.9788 Å, maximal $\Delta f'$), and at a remote wavelength (λ_0 = 0.9711 Å). The diffraction images were indexed and integrated by using the program DENZO (19). The integrated reflections were scaled by using the program SCALEPACK (19). Structure factors amplitudes were calculated by using TRUNCATE from the CCP4 program suite (20). Details of the data collection are described in Table 1.

Multiple-Wavelength Anomalous Diffraction Phasing. Selenium sites were identified with SHAKE 'N BAKE (21) by using data collected at the selenium absorption peak and SOLVE (22) for all three wavelengths. D-LDH contains 14 Met residues per monomer, two of which are at positions 1 and 4 at the N terminus, which might be mobile and hence not visible. Therefore, we expected at least 24 selenium sites in the asymmetric unit, but only 16 could be identified. Residual maps calculated from the phases of the 16 sites failed to locate the remaining SeMet sites. The initial density map was improved by density modification by using DM as implemented in the CCP4 program suite (20). By inspection of the selenium positions by using FINDNCS (23), a nonproper noncrystallographic axis (α = 92.88°, β = 18.28°, γ = 269.25°) could be identified and corresponded to the self-rotation function calculated on the SeMet peak data by using AMORE (24). Noncrystallographic symmetry averaging by using this operator slightly improved the density-modified map.

Table 2. Statistics of the refinement of the atomic model of D-LDH to x-ray diffraction data

Resolution range	20 − 1.9, Å
Protein atoms	8,533
Solvent atoms	392
Unique reflections	76,528
R_{work}*	20.1, %
R_{free}†	24.5, %
rms deviation bond lengths	0.024, Å
rms deviation bond angles	2.43°
rms deviation between NCS related molecules	0.32, Å

*$R_{work} = \Sigma_{(h,k,l)} ||F_o| - |F_c|| / \Sigma_{(h,k,l)} |F_o|$, where F_o and F_c are the observed and calculated structure factors, respectively.

†$R_{free} = \Sigma_{(h,k,l)\varepsilon T} ||F_o| - |F_c|| / \Sigma_{(h,k,l)\varepsilon T} |F_c|$, where T is the test set containing a randomly selected 10% of the observed reflections omitted from the refinement process.

Model Building and Structure Refinement. Electron densities of both averaged and unaveraged maps were used to build the model with the program O (25). Atomic refinement was carried out with the program CNS (26), by using cycles of simulated annealing, energy minimization, and refinement of individual temperature factors. Calculations of overall anisotropic temperature factors, bulk solvent correction, and noncrystallographic symmetry restraints were used throughout. In each round of model building, σa-weighted (27), $2F_{obs} - F_{calc}$, and $F_{obs} - F_{calc}$ maps were calculated. Refinement moves were accepted only when they produced a decrease in the R_{free} value. In later rounds of refinement, water molecules were built into peaks greater than 3σ in $F_{obs} - F_{calc}$ maps.

During model building, it became clear that a ≈50 residue portion of the D-LDH structure is disordered. The disordered region exhibits electron density that is discontinuous and untraceable in both the original multiple-wavelength anomalous diffraction electron density map and the final refined maps. These results are consistent with SHAKE 'N BAKE, SOLVE, and residual maps that revealed only 8 of the 12 SeMet sites per monomer. The current model contains residues 9–328, 375–567, an acetate molecule, a FAD molecule, and ≈200 water molecules per monomer. The two monomers are essentially identical, with rms deviation of 0.3 Å for all C_α atoms. The R_{free} value is 24.7% (for the 10% of the reflections not used in the refinement), and the R_{work} value is 20.0% for all data to 1.9 Å. A total of 88% and 11.5% of backbone $\phi\psi$ conformations are respectively within the most favored and additionally allowed regions of the Ramachandran plot, and only one residue (Ala-74) lies in the disallowed region, as assessed with PROCHECK (28). Refinement statistics for the D-LDH structure are shown in Table 2. The D-LDH model was evaluated with the program VERIFY3D (29), showing normal behavior, and with ERRAT (30), which shows that only 2.9% of the residues are outside the ERRAT 95% confidence limit.

Results

Overall Structure. The D-LDH structure is composed of three discontinuous domains: the FAD-binding domain (residues 1–268 and 520–571), the cap domain (residues 269–310, 388–425, and 450–519), and the membrane-binding domain (residues 311–387 and 426–449, of which residues 329–376 are in the disordered region) (Fig. 1). The FAD-binding domain consists of two $\alpha + \beta$ subdomains; one is composed of three antiparallel β strands surrounded by five α helices and is packed against the second subdomain containing five parallel β strands surrounded by four α helices. The cap domain consists of a large seven-stranded antiparallel β sheet flanked on both sides by α helices. The membrane-binding domain is composed of four α helices.

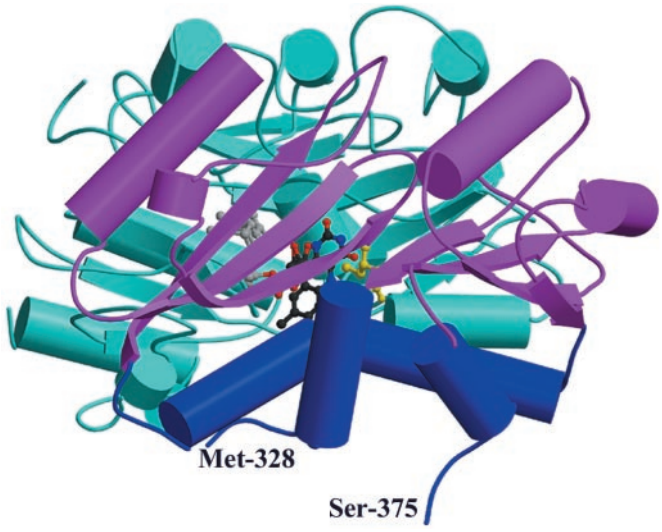

Fig. 1. Ribbon representation of the D-LDH molecule complexed with FAD. The three domains are: in cyan, the FAD-binding domain; in purple, the cap domain; and in blue, the membrane-binding domain. The 50 missing residues from the membrane-binding domain lie between Met-328 and Ser-375. The stick drawing of the cofactor is depicted with gray balls for atoms in the adenine and sugar rings, with red balls for phosphate and oxygen atoms, and with black balls for atoms of the isoalloxazine ring. The active site residues are shown in yellow (Ile-142 and Ser-144). Figure created by MOLSCRIPT (38) and RASTER3D (39, 40).

Contacts at the interface between the FAD-binding and cap domains include hydrophobic and polar interactions, as well as two salt bridges (Arg-40–Asp-498 and Arg-136–Glu-271) situated at the extremities of the surface. The interface between the cap and membrane-binding domains is formed by the packing of β sheets against α helices and is dominated by hydrophobic and a few polar interactions. The interface between the FAD and membrane-binding domains consists solely of the interaction of Leu-327 with Phe-39.

The two subdomains of the FAD-binding domain accommodate the FAD cofactor between them. They envelop most of the FAD cofactor and interact with it by hydrogen bonds and van der Waals contacts. The isoalloxazine ring of the FAD molecule lies at the juncture of the three domains, although the cap and the membrane-binding domains have no direct interaction with it.

Comparison to Other Members of the FAD Family. Screening the database with the D-LDH sequence by using the BLAST (31) profile-based approach and multiple alignment program (32) revealed, as reported previously, that D-LDH belongs to a recently discovered family of FAD-dependent proteins that share a conserved FAD-binding domain (16). Some of the family members are MurB (18), a flavoenzyme involved in the biosynthesis of the bacterial cell wall, PCMH (17), a flavocytochrome c, and vanillyl-alcohol oxidase (16). Although the sequence identity between D-LDH and these proteins, along the entire alignment, is less than 15%, they share some conserved residues in the N-terminal region comprising part of the FAD-binding domain (a multiple sequence alignment is available as supplementary Fig. 5 in the supplementary material; see www.pnas.org). Some of the conserved residues are directly involved in binding the FAD cofactor, and the rest are in the vicinity of the binding site. As a result, the structure of the FAD-binding domain is homologous in all these proteins as indicated by the program DALI (33) and is distinguished from the Rossmann fold (34). This structural similarity is observed, to a lesser extent, in the cap domain, although there is no apparent sequence similarity.

The most significant conformation difference among these structures is in the membrane-binding domain. This is illustrated by the superposition of the D-LDH structure onto that of PCMH, which reveals that the rms deviation is $\approx$2.3 Å for 470 Cα atoms from the FAD-binding domain and the cap domain (Fig. 2 *a* and *b*) and $\approx$4.4 Å for 50 Cα atoms from the membrane-binding domain (Fig. 2*c*). More interestingly, the comparison of the structures of D-LDH and MurB reveals that the topologies of the cap and FAD-binding domains are similar, but that MurB is missing the membrane-binding domain (Fig. 2*d*).

FAD Binding. Except for the dimethylbenzene part of the isoalloxazine ring system, most FAD atoms are solvent inaccessible, forming van der Waals contacts and hydrogen bonds to residues in the FAD-binding domain. Some of the FAD atoms form hydrogen bonds to a few water molecules (Fig. 3). The van der Waals interactions are solely with the flavin ring of FAD, specifically from residues Leu-**81**, Ile-147, Phe-39, Ser-144, Glu-528, and His-529, where the bold residue number indicates conserved residues in the FAD-binding domain. The flavin ring accepts hydrogen bonds from the NH groups of Gly-160 and Gly-143 and from a water molecule. The remaining interactions are hydrogen bonds donated by the peptide NH groups of residues Thr-**79**, and Ser-150, and by the O atoms of Ser-**85**, Ser-150, and Thr-**79**, as well as to two water molecules. One of the highly conserved regions in the FAD-binding domain includes residues **75–85**, which play a major role in FAD binding (see supplementary Fig. 5 in the supplementary material at www.pnas.org). Some of these are directly hydrogen bonded to the FAD molecule, and the rest are in the binding area.

Extra Density. The electron density map of D-LDH shows a strong peak, $\approx 8\sigma$, approximately 3.6 Å from the flavin part of FAD. It is too large to be a water molecule and has been assigned to an acetate ion, as acetate is present in the crystallization conditions. The acetate molecule is hydrogen bonded to the side chain of His-496 (cap domain), Arg-434 (membrane-binding domain), and His-529 (FAD-binding domain).

Discussion

Catalytic Center. Although the position of the active site is unknown, some evidence (G. R. Matcuk, Jr., E.A.P., and C.H., unpublished results) suggests it is located close to the isoalloxazine ring of FAD in the neighborhood of residues 139–144. These residues, particularly Ile-142 and Ser-144, have hydrophobic interactions with the flavin ring (Fig. 3) and are part of the FAD-binding domain. They are also close to the interface of the three domains, which raises the possibility that the binding site on the protein for the substrate and FAD involves all three domains (Fig. 1). Furthermore, the D-lactate-binding site is close to the dimethylbenzene part of the isoalloxazine ring, which is solvent accessible and could guide the approach of the substrate to the active site for maximal catalytic efficiency. This solvent accessibility of the dimethylbenzene ring of the flavin also suggests a possible site for electron transfer to the quinone, which in turn transfers electrons to membrane proteins in the respiratory chain.

Membrane-Binding Domain. ^{19}F-NMR spectroscopy studies have been carried out (12–15) on wild-type D-LDH and mutants in which an additional 5F-tryptophan was substituted at selected positions. These studies indicate that the membrane-binding domain appears to include the segment between Tyr-228 and Phe-369 but is not continuous within this segment. Specifically, the resonances of residues Tyr-228, Phe-279, Tyr-280, Tyr-309, Tyr-321, Phe-339, Phe-340, Phe-341, Phe-356, Phe-357, Phe-361, and Phe-369 were found to be broadened by a nitroxide-spin-labeled fatty acid incorporated into the lipid phase used to

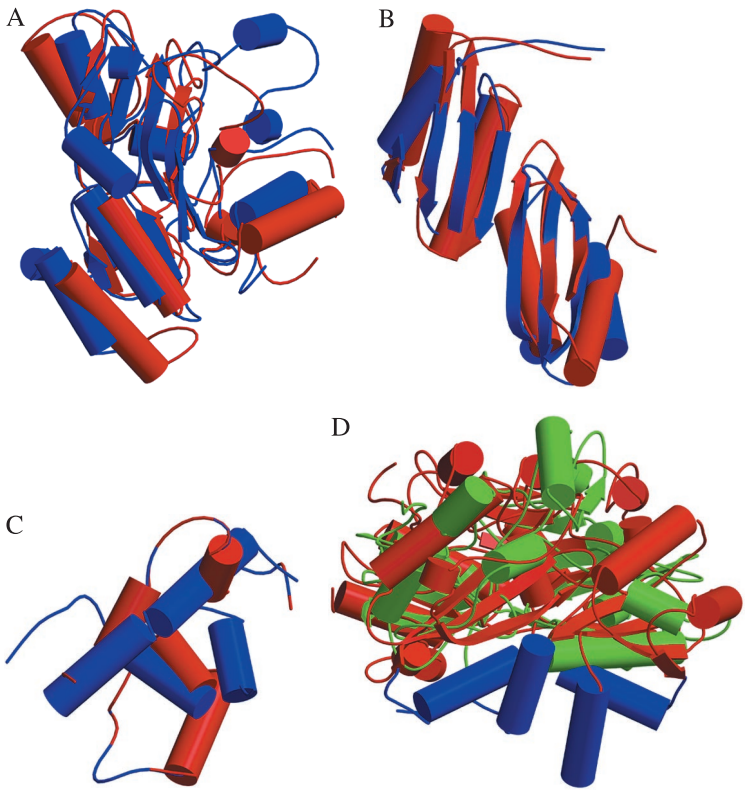

Fig. 2. Comparison of the three individual domains of D-LDH with the corresponding domains of PCMH and MurB. (*A*) The FAD-binding domains of D-LDH (blue) and PCMH (red). (*B*) The cap domains of D-LDH (blue) and PCMH (red). (*C*) The membrane-binding domain of D-LDH and the corresponding region in PCMH. (*D*) The overall structure of D-LDH (FAD and cap domains in red and the membrane-binding domain in blue) compared with MurB (green). The ribbon representation shows the general similarity of the FAD and cap domains of D-LDH to those of MurB or PCMH. The membrane-binding domain is absent in MurB and differs significantly in PCMH.

solubilize D-LDH. Based on our D-LDH structure, the last eight of these are in fact in the membrane-binding domain, but residue 228 belongs to the FAD-binding domain and is in fact exposed to the solvent, and residues 279, 280, and 309 belong to the cap domain. Residues 280 and 309 form hydrogen bonds with residues in the membrane-binding domain and are in fact in the interface between the two domains. Furthermore, residues 280 and 309 are within 15–20 Å of the membrane, which is in the range of the effect of nitroxide-spin-label on the ^{19}F resonance. Residue 279, postulated (13) to be close to the lipid phase, belongs to the cap domain, and, in the model below, is close to the membrane.

Association with the Membrane. The residues in the membrane-binding domain show an excess of basic (19) over acidic (10), with a significant electropositive surface potential flanking the membrane-binding domain surface (35). This electropositive surface is comprised of residues Arg-312, Arg-380, Lys-382, Arg-385, Lys-429, and Arg-443, which are part of the observed structure. These positive residues are distributed evenly in the membrane-binding domain and are contributed from all four α helices and one loop. Their side chains point away from the protein core in the same general direction (blue balls in Fig. 4). Apart from residues Arg-385 and Arg-380, these positive charges are not compensated by hydrogen bonds to negatively charged residues on the protein surface. More interestingly, there are ≈200 water molecules per monomer, which are evenly distributed around the FAD-binding domain and the cap domain, but none of which make hydrogen bonds to residues from the membrane-binding domain. The presence of positive residues lacking hydrogen bonds to acidic residues, or to water molecules, and the absence of lipids or detergents (detergents were not included in the crystallization conditions), permit these residues to be mobile. This is shown by the high average B-factor observed for the membrane-binding domain (≈44 Å^2 for 50 residues) compared with the more usual value found for the other two domains (≈20 Å^2 for 470 residues).

We propose a model for the association of D-LDH to the membrane. We note that there are nine other positive residues

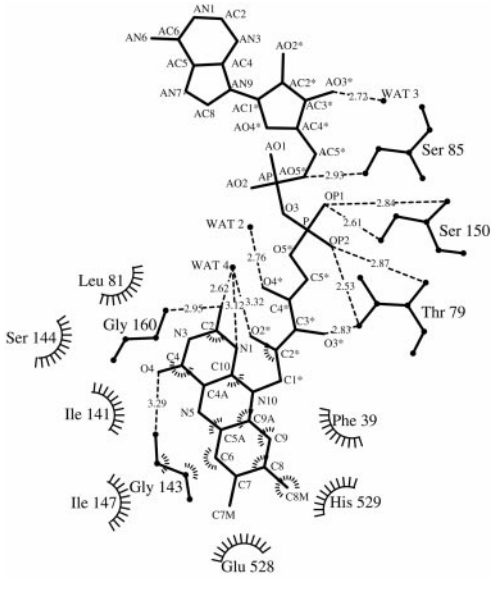

Fig. 3. Schematic diagram of D-LDH interactions with the FAD cofactor was created by using the program LIGPLOT (42). All van der Waals interactions and hydrogen bond contacts to the FAD cofactor (*Middle*) are contributed solely from residues of the FAD-binding domain. The residues that form hydrogen-bonds to the FAD are shown in ball-and-stick representation. Hydrogen bonds are presented as dashed lines and the interatomic distances are shown in angstroms. The residues that form van der Waals contacts with the FAD are depicted as labeled arcs with radial spokes that point toward the ligand atoms with which they interact.

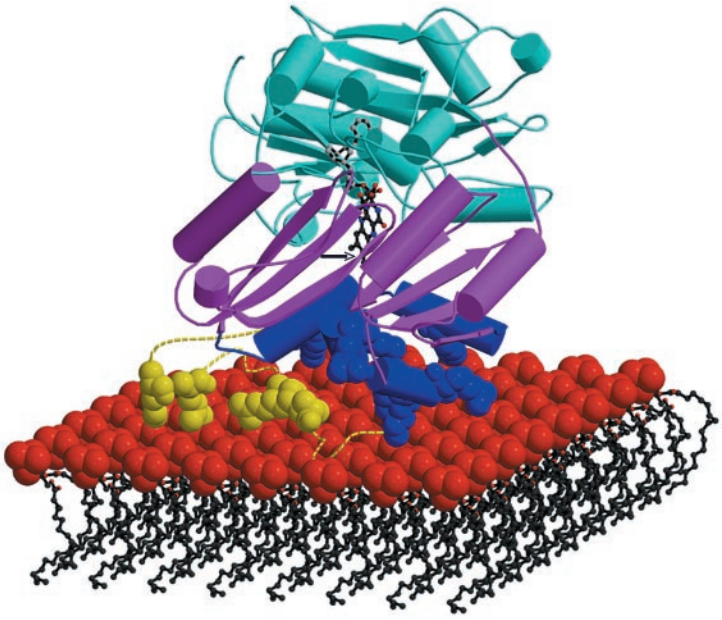

Fig. 4. Cartoon of D-LDH associating with the membrane. D-LDH is anchored to the membrane by electrostatic interactions between basic residues (blue balls) from the observed membrane-binding domain (blue) and possibly from the modeled missing segment (dashed yellow) comprising nine basic residues (yellow balls) and the negatively charged phospholipid head groups (red balls) of the membrane. The cap domain (pink) and FAD-binding domain (cyan) are also shown. The stick drawing of the FAD cofactor is depicted with gray balls for atoms in the adenine and sugar rings, with red balls for phosphate and oxygen atoms, and with black balls for atoms in the isoalloxazine ring. In this model, the substrate D-lactate can approach the active site (as shown by the black arrow) near the isoalloxazine ring (visible between pink strands) from behind the cap domain.

(Lys-331, Lys-336, Lys-344, Arg-346, Lys-353, Lys-355, Arg-358, Arg-364, and Lys-368) in the membrane-binding domain but not modeled in the discontinuous density map. These are shown as yellow balls in Fig. 4. A possible explanation for this disordered segment may be the absence of detergent or lipid in the crystallization solution. That is, this region may not have a defined structure until it binds the membrane, or it may have a defined structure but with several orientations with respect to the rest of the molecule. Therefore, we propose that positive residues, both from the observed structure and possibly from the missing segment, facilitate the interaction of D-LDH with the negatively charged phosphate groups of the phospholipid membrane. This complementary electrostatic interaction presumably would stabilize the orientation of the protein on the membrane surface. Our model for protein–membrane association is supported by previous studies showing that D-LDH in the presence of detergents containing charged head groups, such as hexadecyltrimethylammonium bromide and lysophosphatidylcholine, has a better defined structure than in the presence of nonionic detergent (octyl glucoside) (36). In fact, other peripheral membrane proteins are known to contain clusters of basic residues that facilitate membrane adsorption (2, 3). This observation is reinforced by experimental and theoretical analysis of basic peptide association with membranes containing acidic lipids, suggesting that each basic residue on the protein contributes about 1 kcal/mol to the membrane association energy under physiological conditions (37). D-LDH has at least six and possibly up to fifteen basic residues interacting with the phospholipid head groups, thus contributing at least 6 kcal/mol to the membrane-association energy. This binding energy would compensate for the missing hydrogen bonds of the protein to acidic residues or to water molecules.

A putative model of the 50 missing residues (329–374) (yellow segment in Fig. 4), was built to attach both ends to the structure (residues 328 to 329 and 374 to 375) (blue segment in Fig. 4). This model seems reasonable, given that the solvent content of the crystal is small (30%), which results in tight crystal packing of symmetry-related molecules, especially in the vicinity of the missing residues, constraining the model of this segment. Many alternate orientations were tested but were ruled out because of geometric clashes imposed by symmetry related protein molecules. On the basis of the modeled segment, it is conceivable that several other basic residues might contribute to the electropositive surface of the membrane-binding domain. A model of D-LDH associated with the membrane is presented in Fig. 4. Previous studies (12–15) have shown that residues Phe-339, Phe-340, Phe-341, Phe-356, Phe-357, and Phe-361, among others, are likely to be close to the lipid phase. These residues are part of the modeled region and lie within 7–12 Å of the membrane. This distance is in the range detected by ^{19}F-NMR of nitroxide-spin-labeled fatty acids (15 Å).

Another mechanism proposed for association of peripheral membrane proteins with the membrane is through a mixture of hydrophobic and electrostatic interactions (4, 5). The membrane-binding domain of D-LDH contains 16 apolar residues, nine in the observed structure and seven in the disordered region. Notably, all of the nine residues in the observed structure are distributed on a surface close to the cap domain and away from the membrane-binding surface. Furthermore, inspection of the modeled region suggests that six of its seven apolar residues are positioned in the surface close to the cap domain as well. Apparently D-LDH does not contain membrane-integrating apolar loops or subunits. This observation further supports our interpretation that electrostatic interactions on the membrane surface, rather than a mixture of hydrophobic and electrostatic interactions with the membrane, account for D-LDH-membrane association. Our model is consistent with the previous observation that 0.6 M guanidine hydrochloride is sufficient to elute D-LDH from the *E. coli*. membrane (10), implying that the enzyme does not contain an integral membrane-binding subunit. This model is further supported by the observation that D-LDH retains its solubility and enzymatic activity after detergent (Triton X-100) is removed in the final steps of purification.

The membrane-binding domain (residues 311–387 and 426–449) anchors the protein to the membrane and orients the active site of the enzyme and the solvent-accessible part of the FAD (dimethylbenzene of the isoalloxazine ring) toward the membrane. This orientation appears optimal for electron transfer to a quinone molecule approaching the active site of D-LDH, which subsequently transfers electrons to the membrane. The orientation of D-LDH against the membrane seems suitable for the biological function of the protein.

Conclusions

The structure of D-LDH presented here is the first structure of a peripheral membrane protein from the respiratory chain.

D-LDH is one of the newly discovered family of FAD-containing proteins that share only a few conserved residues in the FAD-binding domain and yet have similar structures in their FAD and cap domains. The major structural difference of D-LDH compared with other family members lies in the membrane-binding domain of D-LDH, which is composed of basic residues evenly distributed on its external surface and hydrophobic residues in the interior. Most of these basic residues are not compensated by hydrogen bonds either to negatively charged residues from the protein or to water molecules, and their side chains point to the exterior of the protein. The fact that the apolar residues are located in the protein interior rules out the model in which apolar loops on the exterior of the protein penetrate the membrane. Therefore, D-LDH association with the membrane is most likely through electrostatic interactions between the electropositive surface of the protein and the electronegative phospholipid head groups of the membrane. Although the current structure fails to disclose part of the membrane-binding domain, the evidence suggests an interaction between an electropositive surface of D-LDH with negative phospholipid head groups. This electrostatic interaction is consistent with other structures of peripheral membrane proteins, which were found to interact with the membrane in a similar manner (2, 3).

We thank Drs. Duilio Cascio, Ken Goodwill, Zhen-Yu Sun, and Ioannis Xenarios for discussions. This research was supported in part by the Alexander Hollaender Distinguished Postdoctoral Fellowship to O.D. and was sponsored by the United States Department of Energy and the National Institutes of Health.

1. Singer, S. J. & Nicholson, G. L. (1972) *Science* **175,** 720–731.
2. Lloyd, S. A., Whitby, F. G., Blair, D. F. & Hill, C. P. (1999) *Nature (London)* **400,** 472–475.
3. Stams, T., Chen, Y., Boriack-Sjodin, P. N., Hurt, J. D., Liao, J., May, J. A., Deen, T., Laiplis, P., Silverman, D. N. & Christianson, D. W. (1998) *Protein Sci.* **7,** 556–563.
4. Picot, D., Loll, P. J. & Gravito, M. (1994) *Nature (London)* **367,** 243–249.
5. Macedo-Ribeiro, S., Bode, W., Huber, R., Quinn-Allen, M. A., Kim, S. W., Ortel, T. L., Bourenkov, G. P., Bartunik, H. D., Stubbs, M. T., Kane, W. H., *et al.* (1999) *Nature (London)* **402,** 434–439.
6. Futai, M. (1992) *Biochemistry* **12,** 2468–2474.
7. Kohn, L. D. & Kaback, H. R. (1973) *J. Biol. Chem.* **248,** 7012–7017.
8. Tanaka, Y., Anraku, Y. & Futai, M. (1976) *J. Biochem.* **80,** 821–830.
9. Pratt, E. A., Fung, L. W.-M., Flowers, J. A. & Ho, C. (1979) *Biochemistry* **18,** 312–316.
10. Reeves, J. P., Hong, J.-S. & Kaback, H. R. (1973) *Proc. Natl. Acad. Sci. USA* **70,** 1917–1921.
11. Sun, Z.-Y., Dowd, S. R., Felix, C., Hyde, J. S. & Ho. C. (1995) *Biochim. Biophys. Acta* **1252,** 269–277.
12. Peersen, O. B., Pratt, E. A., Truong, H.-T. N., Ho, C. & Rule, G. S. (1990) *Biochemistry* **29,** 3256–3262.
13. Sun, Z.-Y., Truong, H.-T. N., Pratt, E. A., Sutherland, D. C., Kulig, C. E., Homer, R. J., Groetsch, S. M., Hsue, P. Y. & Ho, C. (1993) *Protein Sci.* **2,** 1938–1947.
14. Dowd, S. R., Pratt, E. A., Sun, Z.-Y. & Ho, C. (1995) *Biochim. Biophys. Acta* **1252,** 278–283.
15. Sun, Z.-Y., Pratt, E. A. & Ho, C. (1996) *Biomedical Frontiers of Fluorine Chemistry*, ACS Symposium Series, eds. Ojima, I., McCarthy, J. R. & Welch, J. T. (Am. Chem. Soc., Washington, DC), Vol. 639, 296–310.
16. Mattevi, A., Fraaije, M. W., Mozzarelli, A., Olici, L., Coda, A. & Berkel, W. J. H. (1997) *Structure (London)* **5,** 907–920.
17. Mathews, F. S., Chen, Z.-W. & Bellamy, H. D. (1991) *Biochemistry* **30,** 237–247.
18. Benson, T. E., Filman, D. J., Walsh, C. T. & Hogle, J. M. (1995) *Nat. Struct. Biol.* **2,** 644–653.
19. Ottwinowski, Z. & Minor, W. (1997) *Methods Enzymol.* **276,** 307–326.
20. Collaborative Computational Project No. 4 (1994) *Acta Crystallogr. D* **50,** 760–763.
21. Smith, G. D., Nagar, B., Rini, J. M., Hauptman, H. A. & Blessing, R. H. (1998) *Acta Crystallogr. D* **54,** 799–804.
22. Terwilliger, T. C. & Berendzen, J. (1999) *Acta Crystallogr. D* **55,** 849–861.
23. Lu, G. (1999) *J. Appl. Crystallogr.* **32,** 365–368.
24. Navaza, J. (1994) *Acta Crystallogr. A* **50,** 157–163.
25. Jones, T. A., Zou, J. Y., Cowan, S. W. & Kjeldgaard, M. W. (1991) *Acta Crystallogr. A* **47,** 110–119.
26. Brunger, A. T., Adams, P. D., Clore, G. M., DeLano, W. L., Gros, P., Grosse-Kunstleve, R. W., Jiang, J. S., Kuszewski, J., Nilges, M., Pannu, N. S., *et al.* (1998) *Acta Crystallogr. D* **54,** 905–921.
27. Read, R. J. (1986) *Acta Crystallogr. A* **42,** 140–149.
28. Laskowski, R. A., MacArthur, M. W., Moss, D. S. & Thornton, J. M. (1993) *J. Appl. Crystallogr.* **26,** 283–291.
29. Luethy, R., Bowie, J. U. & Eisenberg, D. (1992) *Nature (London)* **356,** 83–85.
30. Colovos, C. & Yeates, T. O. (1993) *Protein Sci.* **2,** 1511–1519.
31. Altschul, S. F., Gish, W., Miller, W., Myers, E. W. & Lipman, D. J. (1990) *J. Mol. Biol.* **215,** 403–410.
32. Bucher, P., Karplus, K., Moeri, N. & Hofmann, K. (1996) *Comput. Chem.* **20,** 3–23.
33. Holm, L. & Sander, C. (1993) *J. Mol. Biol.* **233,** 123–138.
34. Rossmann, M. G., Liljas, A., Branden, C.-I. & Banaszak, L. J. (1975) *Enzymes* **11,** 61–102.
35. Nicholls, A., Sharp, K. & Honig, B. (1991) *Proteins Struct. Funct. Genet.* **11,** 281–291.
36. Sun, Z.-Y., Pratt, E. A., Simplaceanu, V. & Ho, C. (1996) *Biochemistry* **35,** 16502–16509.
37. Ben-Tal, N., Honig, B., Peitzsch, R. P., Denisov, G. & McLaughlin, S. (1996) *Biophys. J.* **71,** 561–575.
38. Kraulis, P. J. (1991) *J. Appl. Crystallogr.* **24,** 946–950.
39. Bacon, D. J. & Anderson, W. F. (1988) *J. Mol. Graphics* **6,** 219–220.
40. Merrit, E. A. & Murphy, M. E. P. (1994) *Acta. Crystallogr. D* **50,** 869–873.
41. Higgins, D. G., Thompson, J. D. & Gibson, T. J. (1996) *Methods Enzymol.* **266,** 383–402.
42. Wallace, A. C., Laskowski, R. A. & Thornton, T. M. (1995) *Protein Eng.* **8,** 127–134.